Crystals **2012**, *2*, 446-465; doi:10.3390/cryst2020446

OPEN ACCESS

crystals

ISSN 2073-4352

www.mdpi.com/journal/crystals

Article

Synthesis, Structure and Solid State Properties of Cyclohexanemethylamine Substituted Phenalenyl Based Molecular Conductor

Pradip Bag [1], Mikhail E. Itkis [1], Sushanta K. Pal [1], Elena Bekyarova [1], Bruno Donnadieu [1] and Robert C. Haddon [1,2,*]

[1] Department of Chemistry, University of California, Riverside, CA 92521-0403, USA; E-Mails: pradipb@ucr.edu (P.B.); mitkis@engr.ucr.edu (M.E.I.); sushanta@ucr.edu (S.K.P.); elena.bekyarova@ucr.edu (E.B.); bruno.donnadieu@ucr.edu (B.D.)

[2] Department of Chemical and Environmental Engineering, University of California, Riverside, CA 92521-0403, USA

* Author to whom correspondence should be addressed; E-Mail: haddon@ucr.edu; Tel.:+1-951-827-2233; Fax: +1-951-827-2233.

Received: 30 March 2012; in revised form: 20 April 2012 / Accepted: 2 May 2012 / Published: 14 May 2012

Abstract: We report the preparation, crystallization and solid state characterization of a cyclohexanemethylamine substituted spirobiphenalenyl radical; in the solid state the compound is iso-structural with its dehydro-analog (benzylamine-substitued compound), and the molecules packed in a one-dimensional fashion that we refer to as a π-step stack. Neighboring molecules in the stack interact via the overlap of one pair of active (spin bearing) carbon atoms per phenalenyl unit. The magnetic susceptibility measurement indicates that in the solid state the radical remains paramagnetic and the fraction of Curie spins is 0.75 per molecule. We use the analytical form of the Bonner-Fisher model for the S = 1/2 antiferromagnetic Heisenberg chain of isotropically interacting spins with intrachain spin coupling constant J = 6.3 cm^{-1}, to fit the experimentally observed paramagnetism [χ_p (T)] in the temperature range 4–330 K. The measured room temperature conductivity (σ_{RT} = 2.4 × 10^{-3} S/cm) is comparable with that of the iso-structural benzyl radical, even though the calculated band dispersions are smaller than that of the unsaturated analog.

Keywords: molecular conductors; phenalenyl; spirobis-phenalenyl boron; neutral radical; 1D conducting pathways

---

1. Introduction

Molecular conductors have been widely explored in the areas of optoelectronics, magnetooptics and spintronics [1–5]. and phenalenyl based radical conductors have been the subject of number recent reviews [6–8]. Phenalenyl (PLY), a polycyclic odd-alternant hydrocarbon with a planar D_{3h} symmetric π-electronic system, is one of the fundamental delocalized neutral radicals [9,10]. Because of its simple and highly symmetric structure, and its intriguing properties in solution and in the crystalline state, it has fascinated researchers for some time [6,7,11,12]. It was first proposed in 1975 that phenalenyl has the potential to serve as a building block for molecular conductors [13–15]. Since then synthetic efforts have led to the crystallization and characterization of several types of PLY derivatives by chemical modification [16–23]. Heteroatom functionalization of neutral radicals such as thio-substituted PLY [24–26], azaphenalenyls [12,27,28], and bisphenalenyl boron complexes [29,30] have played a crucial role in the recent progress in phenalenyl chemistry and the important developments in heterocyclic radicals [31–35].

In our pursuit of phenalenyl-based neutral radical molecular conductors, we have used N- and O-functionalization to create three families of spiro-bis(1,9-disubstituted phenalenyl) boron radicals and one tris(1,9-disubstituted phenalenyl) silicon neutral radical (**1**−**22**, Scheme 1). Unlike conventional neutral radicals, in the solid state the spiro-conjugated biphenalenyls give rise to a quarter-filled energy band, and this significantly reduces the on-site Coulomb correlation energy (U), which is usually responsible for the insulating ground-state that occurs in half-filled band structures.

The first PLY based neutral radical molecular conductor (**5**) [36] was found to be monomeric and it showed Curie behavior throughout the temperature range 10−400 K, thereby confirming the presence of non-interacting spins in the solid state. Nevertheless the compound showed a room-temperature conductivity of σ_{RT} = 0.05 S/cm and the radical was best represented as a degenerate Mott-Hubbard insulator [36]. Similar to **5**, the compounds **16**, **17** and **18** have very weak intermolecular interactions in the solid state, and the magnetic susceptibility could be fit to the Curie−Weiss function with $\theta = -55$ K (**16**), −70 K (**17**), and −14 K (**18**), or to the antiferromagnetic 1D Heisenberg model; the conductivities span a broad range: σ_{RT} = 0.04 (**16**), 0.01 (**17**), and 7×10^{-6} S/cm (**18**) [37]. Shorter chain analogs of **5**, the ethyl (**1**) and butyl (**3**) compounds crystallized as face-to-face π-dimers and showed conductivities of σ_{RT} = 0.01 (**1**), and 0.02 (**3**) S/cm [38]. These dimeric neutral radicals (**1** and **3**) simultaneously exhibit bistability in three physical channels: magnetic, electrical and optical, which has been rarely realized in a single system [39–42]. The crystals undergo phase transitions from high temperature paramagnetic states to low temperature diamagnetic states, accompanied by an increase in the conductivities by 2 orders of magnitude. The radicals **2**, **4** and **13** crystallize as weakly bound, paramagnetic π-dimers but the conductivities of these compounds ($\sigma_{RT} = 1.4 \times 10^{-6}$ S/cm (**2**), 0.4×10^{-6} S/cm (**4**), and 0.5×10^{-6} S/cm (**13**)) are much lower than those of **1** and **3**, because of the orientation of the molecules in the crystal lattice [43,44]. The *n*-octyl (**6**) and cyclooctyl (**10**) radicals can be crystallized as both a σ-dimer and a π-dimer—these latter structures are weakly bound (paramagnetic, **6**) and strongly bound (diamagnetic, **10**) dimers; both compounds show low conductivity: $\sigma_{RT} = 1 \times 10^{-5}$ (**6**), and 1×10^{-6} S/cm (**10**) [45–47].

Scheme 1. Molecular structures of phenalenyl based radicals.

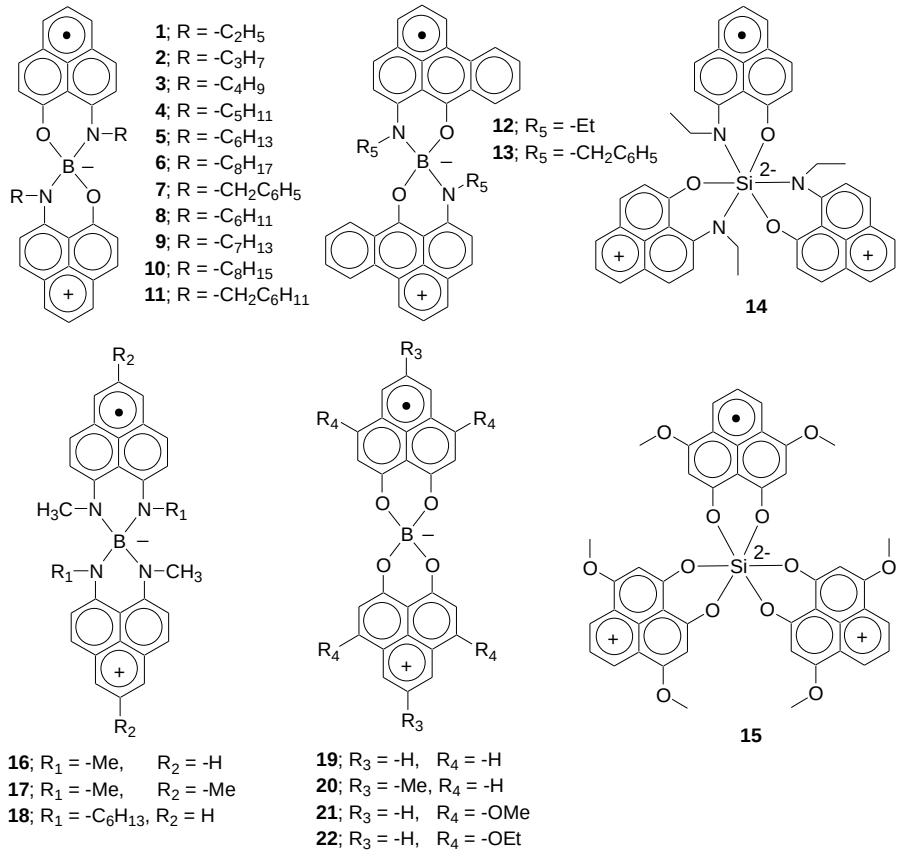

Apart from the structural motifs discussed above we have found a number of 1D- and pseudo-1D-neutral radical conductors; the first of these was the benzyl compound (**7**), which crystallized in an unusual π-step structure involving superimposed overlap of just 4 of the 12 active carbon atoms with a conductivity, σ_{RT} = 1.4 × 10^{-3} S/cm (**7**) [48]. The results are best interpreted in terms of a resonating valence bond (RVB) ground state [29,30,47,49,50] for this compound and this description is also applicable to the π-chain structures found for compounds **8**, **9**, **19**, and **20** [29,51] which essentially crystallize as infinitely repeating forms of the π-dimers **1** and **3**. These compounds were also stable in their highly symmetric 1D structures and gave rise to some of the highest conductivities attained for this class of compounds: σ_{RT} = 0.3 (**8**), 0.1 (**19**), and 0.3 S/cm (**20**) [51]. Recently, we report low ΔE compounds (**21**, **22**) which have intermediate intermolecular interactions in the solid state [52,53]. The magnetic susceptibility could be fit to the Curie−Weiss function with $\theta = -44$ K for **21** and to the antiferromagnetic 1D Heisenberg chain model for **22**; the conductivities span the range: σ_{RT} = 3 × 10^{-3} (**21**) to 2 × 10^{-2} S/cm (**22**).

Thus it is apparent that the multifunctional PLY neutral radical conductors offer a variety of electronic and solid state structures in which the (de)localization of the spin and charge is of paramount importance. In that context we introduced a related substituent at the 9-position in order to study the response of the molecular packing and the solid state properties such as the optical spectrum, conductivity and magnetism. Herein, we report the synthesis, crystallization, and solid state properties of cyclohexanemethyl substituted spiro-biphenalenyl radical, **11**, another member of $[PLY(O,NR)]_2B$ series. The radical was found to be iso-structural with the dehydro benzyl analog and in the solid state the molecules adopt the π-step structure, analogous to that of **7** [48].

2. Results and Discussion

*2.1. Synthesis of Ligand, Preparation and Electrochemical Properties of Radical **11***

The ligand and the radical were synthesized following the same basic procedures that were used to prepare radicals **1**–**10** [48]. We first prepared the chloride salt (**11**$^+$Cl$^-$) reacting the ligand with boron trichloride and then exchanged the counter anion with tetraphenyl borate to achieve the required solubility properties of the salt (Scheme 2). The electrochemical characteristics of **11**$^+$BPh$_4^-$ were examined by cyclic voltammetry and differential pulse voltammetry and it may be seen in Figure 1 that there are two reversible redox couples for the compound (**11**) with half-wave potentials: $E_1^{1/2}$ = −0.87 V and $E_2^{1/2}$ = −1.27 V. Each of these redox couples corresponds to a one-electron reduction process, indicating successive generation of radical and anion (Scheme 3). The disproportionation potential for **11** is −0.40 V ($\Delta E_{2-1} = E_2^{1/2} - E_1^{1/2}$). This disproportionation potential value is comparable with that of the corresponding PLY compounds (**1**–**10**).

Scheme 2. Synthetic route for preparation of radical **11**.

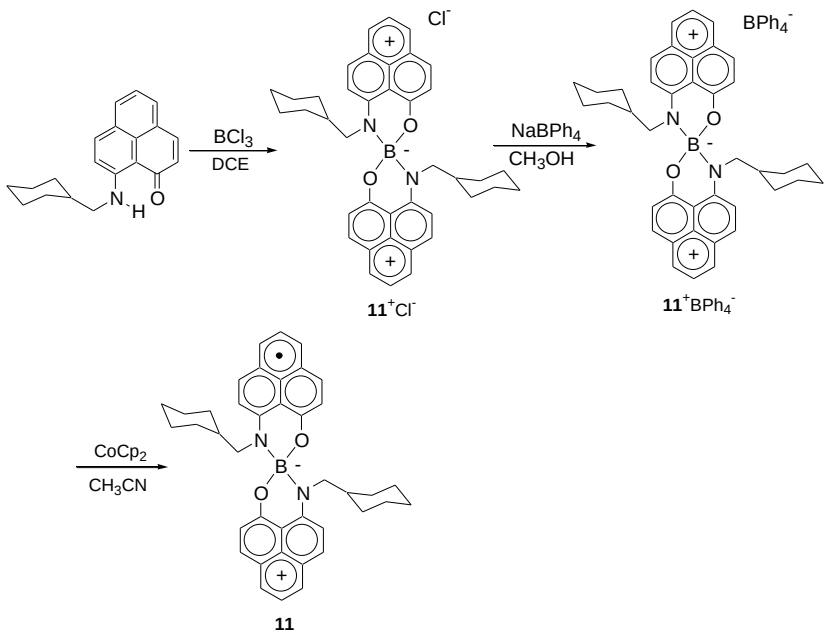

Scheme 3. First and second redox couples.

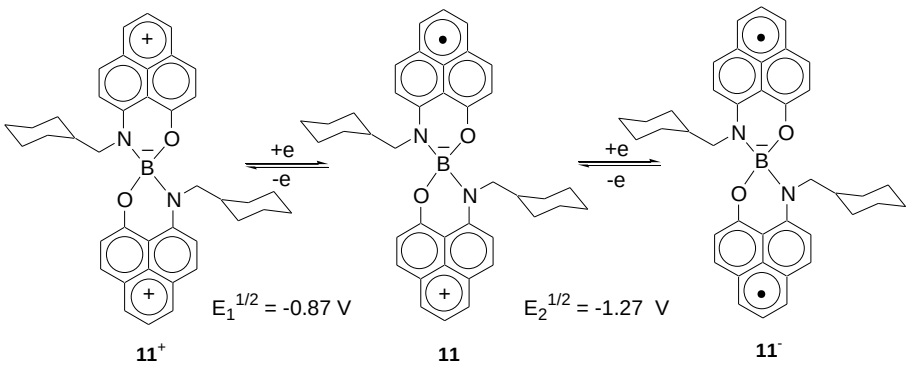

Figure 1. Cyclic voltametry (CV) and differential pulse voltametry (DPV) of **11**$^{+}$BPh$_4^{-}$ in acetonitrile, referenced to SCE via internal reference ferrocene (not shown).

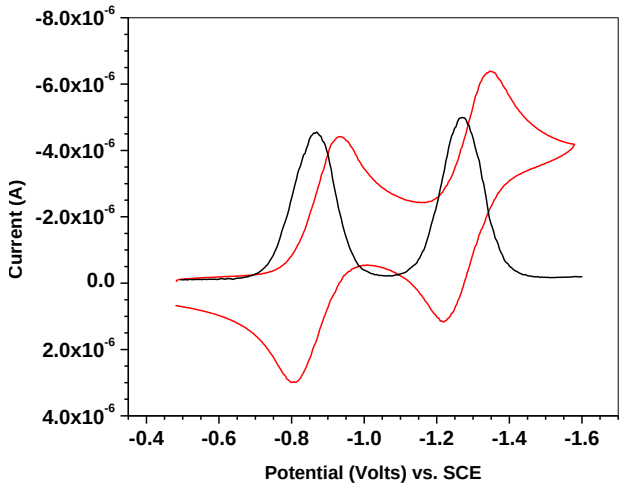

We crystallized the radical **11** by reduction of the corresponding salt (**11**$^{+}$BPh$_4^{-}$) in a vial in glove box using cobaltocene as reducing agent (Scheme 2) [54], and obtained a moderate yield of high quality crystals. Cobaltocene was used as reductant because its oxidation potential ($E^{1/2}$ = −0.91 V) falls between the two reduction potentials of **11**$^{+}$BPh$_4^{-}$. The crystals reached their optimum size and quality in four days. Although solutions of the radical are extremely oxygen sensitive, the crystals are sufficiently stable to obtain elemental analyses, X-ray crystal structures, and other solid state measurements under ambient conditions.

*2.2. X-ray Crystal Structure of **11***

The X-ray crystal structure for compound **11** has been determined at T = 100 K and in the solid state the central boron atom is sitting on a two-fold axis; thus the asymmetric unit contains half of the molecule and there are four molecules of **11** in the unit cell (monoclinic space group C2/c). The crystal data and details of the structure determinations for radicals **11** and **7** are listed in Table 1. An ORTEP drawing of **11** with atom numbering scheme is shown in Figure 2. The structure is similar to the previously reported benzyl analog **7** [48], but different from the recently reported low ΔE_{2-1} radical **22** [53].

Figure 2. ORTEP drawing of the radical **11** with atom numbering scheme.

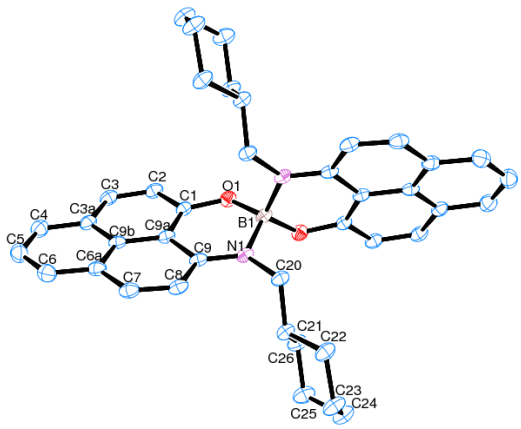

Table 1. Crystal data collection and refinement details for **11** and **7**.

Compound	**11**	**7**
Temperature	100(2) K	223(2) K
Formula	$C_{40}H_{40}BN_2O_2$	$C_{40}H_{28}BN_2O_2$
Formula Weight	591.55	579.45
Crystal System	Monoclinic	Monoclinic
Space group	C2/c	C2/c
a, Å	21.4373(15)	23.386(2)
b, Å	6.1623(4)	5.7326(6)
c, Å	23.2775(16)	20.963(2)
α, degree	90	90
β, degree	97.597 (4)	97.782
γ, degree	90	90
V, $Å^3$	3048(4)	2784.6(5)
Z	4	4
Crystal size, mm^3	0.40 × 0.39 × 0.15	0.55 × 0.19 × 0.17
Theta range for data collection	1.77 to 27.52 °	1.76 to 26.37 °
Reflection collected	19619	8590
Independent reflections	3460	2209
Goodness-of-fit on F^2	1.033	1.038
Final R indices [I > 2sigma(I)]	R1 = 0.0401 wR2 = 0.1005	R1 = 0.0396 wR2 = 0.1027
R indices (all data)	R1 = 0.0607, wR2 = 0.1157	R1 = 0.0524, wR2 = 0.1142

A comparison of relevant crystal parameters pertaining to compounds **7** and **11** (Table 1) reveals that the volume of the unit cell for the radical **11** is higher (3048 $Å^3$) than that of the radical **7** (2784 $Å^3$). A noteworthy structural feature of these compounds (**7** and **11**) is the presence of one dimensional (1D) π-step stacking of phenalenyl units along *y* axis (Figure 3). The packing along other directions (*x* and *z*) is quite different from the packing along the *y* direction but similar in both radicals. The intermolecular short contacts along the *x* axis are 3.54, 3.67 and 4.60 Å for radical **7**, while corresponding contact interactions for radical **11** are 3.70, 4.68 and 4.72 Å respectively (Figure 4). In the *x* and *z* directions the PLY rings are oriented by an angle of 67 °, while in the case of **7** the angle is 80 °. The closest C ··C distances between the angularly oriented phenalenyls in the *xz* plane are 3.70 Å for **11**, 3.54 Å for **7**, higher than the van der Waals distance 3.4 Å.

Along *b* axis the phenalenyl rings on both side of the boron are packed in a π- step fashion as shown in Figures 3 and 5. The closest C ··C distances between molecules along *b* direction are 3.48 and 3.62 Å while that for radical **7** are 3.47 and 3.58 Å (Figure 5). Despite the comparatively large separation the molecules are superimposed at two spin bearing carbons of each phenalenyl unit in **7** (Figure 6), so the overlap between molecules is effective. In radical **11**, there is complete superposition of a pair of spin bearing carbon atoms of the nearest phenalenyl units along the *b* axis, whereas in the case of radical **7** the planes are slightly displaced (Figure 6), for a total of four spin-bearing contacts per molecule.

Figure 3. Packing of the molecules viewed along *b*-axis.

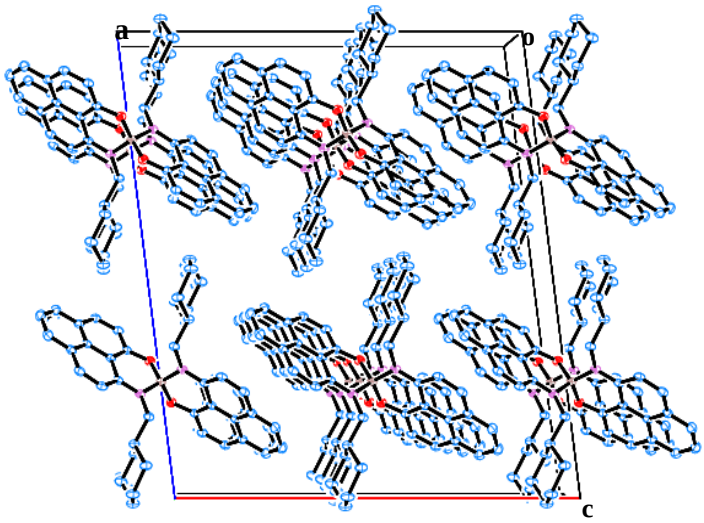

Figure 4. Packing of the molecules in *xz* plane for **7** (**a**) and **11** (**b**). Molecules are viewed along *y* axis, showing the contacts between spin-bearing carbon atoms. Benzyl and cyclohexanemethyl groups are omitted for clarity.

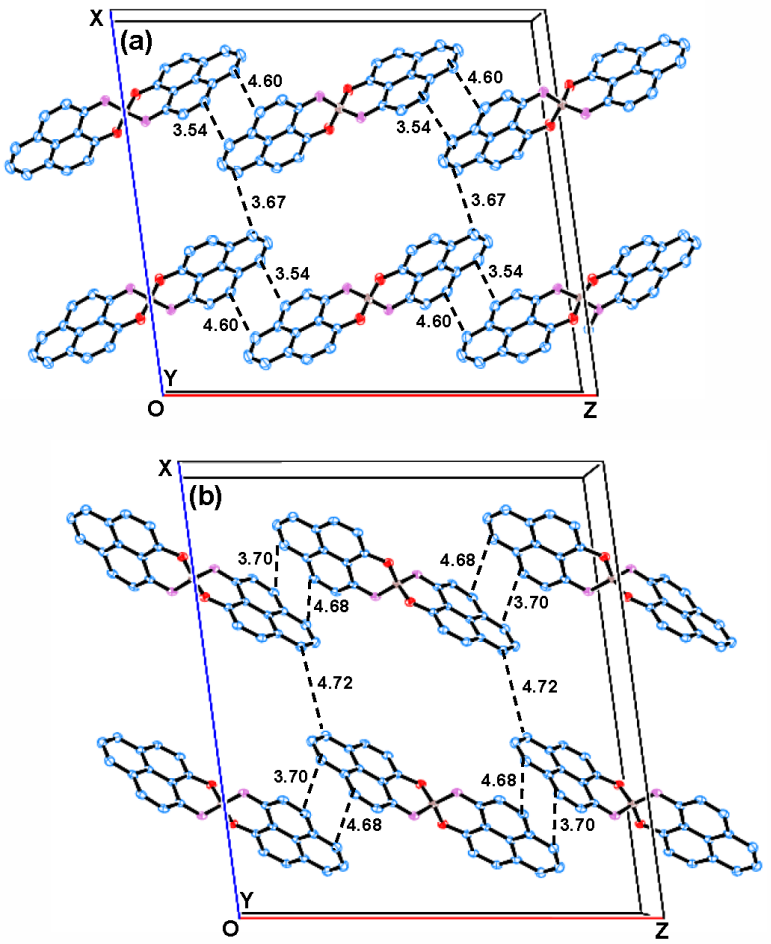

Figure 5. Packing along *b* axis showing one dimensional (1D) π-step structure and the closest intermolecular contacts for **7** (**left**) [48] and **11** (**right**); the four equivalent spin bearing C ··C interactions per molecule are of length 3.47 Å (**7**) and 3.48 Å (**11**). Reprinted with permission from [48] Copyright 2004, American Chemical Society.

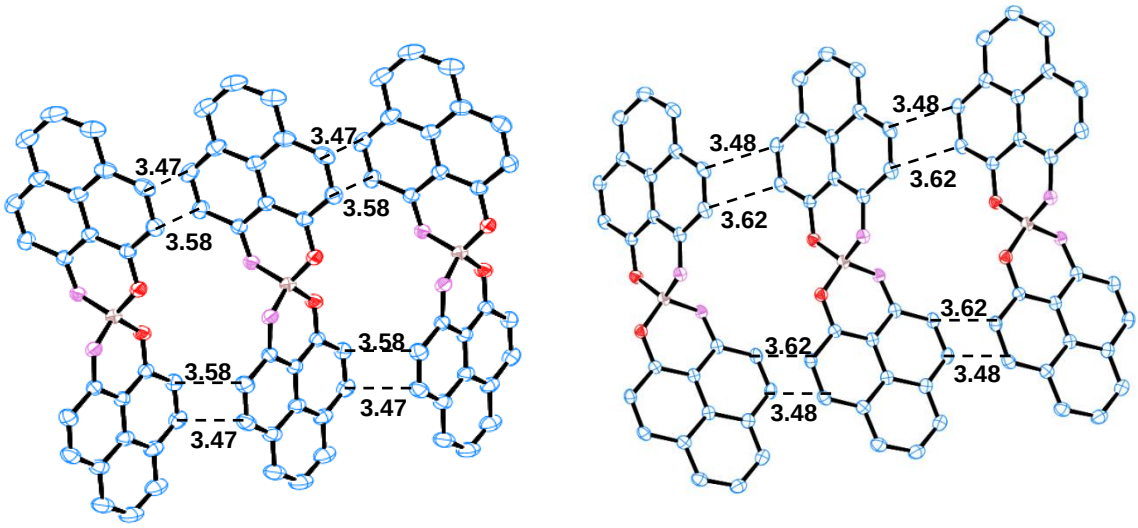

Figure 6. Super-position of a pair of spin bearing carbons per phenalenyl unit (viewed perpendicular to PLY ring) for radicals **7** (**left**) and **11** (**right**). Equivalent superimposed overlaps are observed for total four spin bearing carbons (blue color) per molecule.

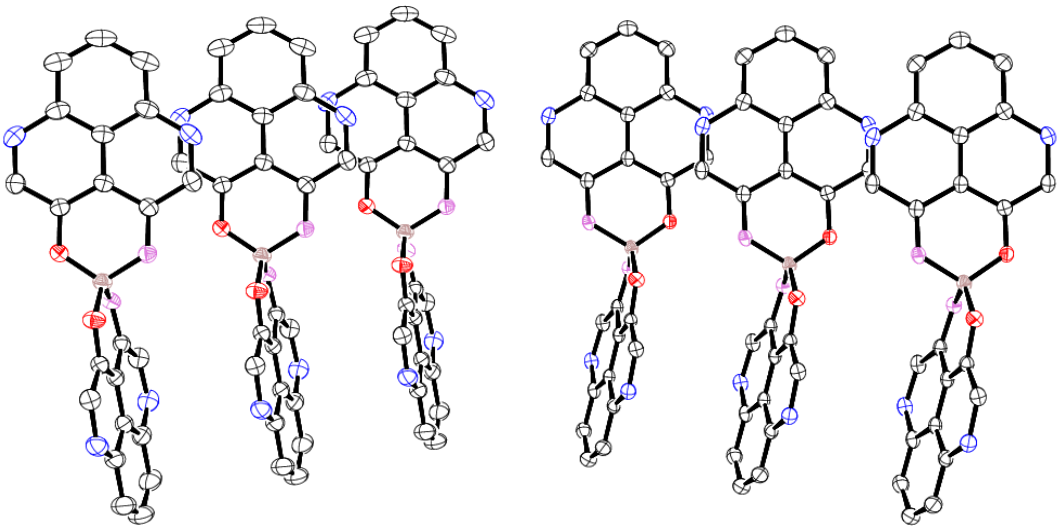

Thus radical **11** exist as a monomeric stack along the *b*-axis (1D) of the unit cell (Figure 4) and all other neighboring PLY units along *a*- and *c*-axis are oriented angularly. There is an effective conducting pathway along *b*-axis in the crystals and the radical is iso-structural with **7**.

*2.3. Magnetic Susceptibility of **11***

The temperature dependence of the magnetic susceptibility (χ) of **11** was measured over the range of 4.4–330 K and is shown in Figure 7a as the paramagnetic susceptibility χ_p after correction for the molecular diamagnetism $\chi_0 = -383.3 \times 10^{-6}$ emu/mol. The measured magnetic susceptibility shows a

Curie-like paramagnetic increase with decreasing temperature which is typical of the phenalenyl-based neutral radical compound **5** although the rate of increase at low temperatures is slower than for a system of non-interacting spins. This deviation from Curie paramagnetism can be clearly seen in Figure 7b where the effective fraction of Curie spins per molecule 8/3 $\times(\chi_p T)$ shows a decrease at low temperatures associated with antiferromagnetic interactions. We used the analytical form of the Bonner-Fisher model for the S = 1/2 antiferromagnetic Heisenberg chain of isotropically interacting spins [55,56], to fit the experimentally observed χ_p (T) in the temperature range 4–330 K. Besides the Bonner-Fisher (BF) contribution the fitting takes into account the paramagnetic impurity term; the analysis gives a concentration of paramagnetic impurities equal to 1.9% Curie spins per molecule, while the remaining Bonner-Fisher (BF) contribution shows a maximum at 12 K corresponding to an intrachain exchange constant, $J = -6.3$ cm^{-1}. Both components are shown in Figure 7a, and their sum satisfactorily matches the experimental χ_p (T) dependence. The uniform Heisenberg model [55,56] is appropriate because of the regular chain structure of **11**, in which the radical spins couple through a single type of π-step interaction.

Figure 7. (**a**) Magnetic susceptibility of **11** as a function of temperature. Red line represents the fitting for magnetic susceptibility of **11** to the Bonner-Fisher model for the S = 1/2 antiferromagnetic Heisenberg chain of isotropically interacting spins which includes the contribution of paramagnetic impurities (dashed line) and Bonner-Fisher (BF) component (black solid line) corresponding to $J = -6.3$ cm^{-1}; (**b**) Fraction of Curie spins per molecule as a function of temperature.

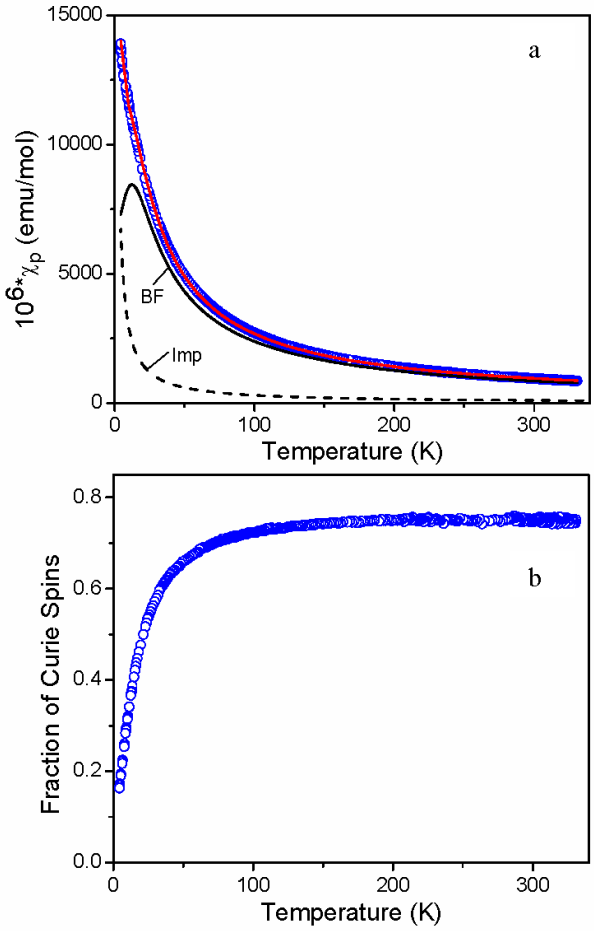

Because compounds **7**, **16** and **17**, also adopt a uniform chain structure we previously used the Bonner-Fisher model for the S = 1/2 antiferromagnetic Heisenberg chain of isotropically interacting spins to fit the respective χ_p (T) values and obtained intra-chain exchange constants $J = -52.3$ cm^{-1} (**7**), −86.0 cm^{-1} (**16**) and −59.0 cm^{-1} (**17**) [48,51], which may be compared to the value of $J = -6.3$ cm^{-1} found in **11**.

*2.4. Conductivity of **11***

The electrical conductivity (σ) of crystalline **11** was measured using four-probe configuration with four in-line contacts placed along the needle axis (Figure S2) over the temperature range from 80 to 330 K (Figure 8). The room-temperature conductivity of **11** was found to be $\sigma_{RT} = 2.4 \times 10^{-3}$ S/cm, slightly higher than the value obtained for the iso-structural radical **7** ($\sigma_{RT} = 1.4 \times 10^{-3}$ S/cm) but less than $\sigma_{RT} = 2 \times 10^{-2}$ S/cm for the low ΔE radical **22**. It may be noted that low value of ΔE_{2-1} (0.23 V) in **22**, is responsible for the one-order increase in the conductivity from that of **7** (0.34 V) and **11** (0.40 V). The conductivity shows a semiconducting temperature dependence with activation energy Δ = 0.22 eV (Figure 8).

Figure 8. Temperature dependence of conductivity of single crystal of radical **11**.

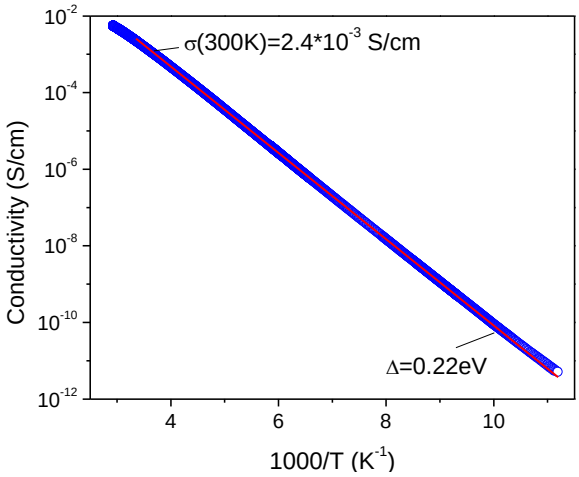

*2.5. Optical Measurement of **11***

Figure 9 represents the single crystal optical spectra of radical **11**. As may be seen in Figure 9, we find an optical energy gap E_g (optical) ≈ 0.50 eV (~ 4000 cm^{-1}) and the spectrum remains opaque past 12,000 cm^{-1} due to band-like excitations that extend through this region of the spectrum. The absorptions in the mid-IR, between 650 and 4000 cm^{-1}, are due to the molecular vibrations of the radical **11**. The nature of the spectra are common to that of other neutral radicals and the optical energy gap E_g is comparable to that of the spiro-biphenalenyl boron radicals reported previously [38,44]. The optical gap is approximately two times higher than the activation energy Δ = 0.22 eV of the electrical conductivity which is similar to the case of conventional intrinsic semiconductors.

Figure 9. Single crystal IR and UV-vis transmission spectra of radical **11**.

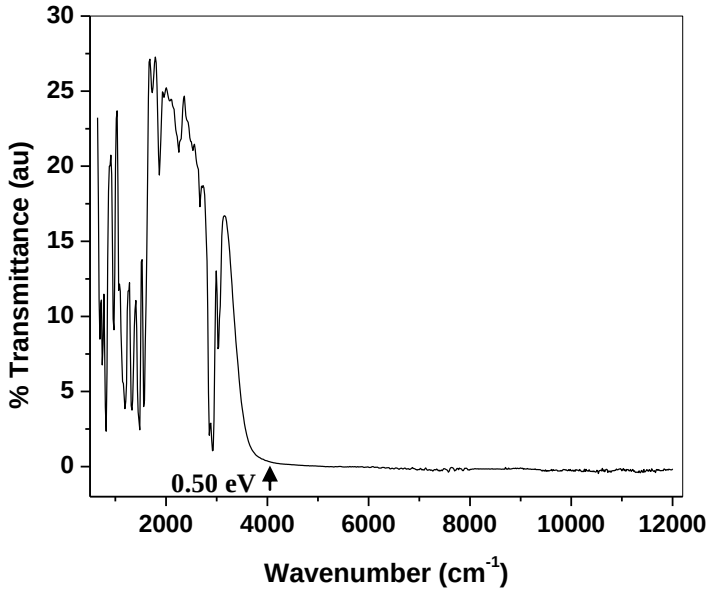

*2.6. Band Electronic Structure of **11***

Figure 10a shows the band structure for the lattice found in the X-ray crystal structure of **11** at 100 K. The eight bands shown in Figure 10a are derived from the two LUMOs of $\mathbf{11}^+$ for each of the four molecules of **11** in the unit cell; these basically consist of symmetric and anti-symmetric combinations of the 1,9-substituted phenalenyl LUMOs. Alternatively, they can be viewed as arising from the non-bonding molecular orbitals of each of the eight phenalenyl units in the unit cell. In the band picture these eight orbitals now accommodate four electrons, leading to a quarter filled band complex with two filled and six vacant bands. As expected, the nature of band structures for **11** at 100 K and **7** at 223 K are similar, because both the compounds are iso-structural with some variation in contact interactions as mentioned in Figures 4,5. There is a substantial band dispersion (0.20 eV) found along π-step direction (*y* axis) in **11** but that for compound **7** is much higher about 0.37 eV, because in **7** spin-bearing C ··C distances are smaller [48]. Dispersions along other directions for both the compounds **7** and **11** are very small and the values are negligibly small for **11** compared to **7**. It may be noted that the low ΔE_{2-1} radical **22** adopts similar kind of π-step structure where the molecules pack in a continuous array of partially π-stacked neighboring PLY units along *b*-axis and similar to the radicals **7** and **11** there are no significant inter-molecular C ··C interactions in **22** (less than 3.4 Å) along other axes. The extended Hückel theory (EHT) predicts that the radical (**22**) has a band dispersion more than 0.5 eV along the packing axis and the room temperature conductivity is 10 times higher than that of radical **7** and **11** [53].

Figure 10. (**a**) Calculated band structures for radical **11** based on X-ray structure at 100 K; (**b**) represents band structure for radical **7** based on structure at 223 K. Reprinted with permission from [48] Copyright 2004, American Chemical Society.

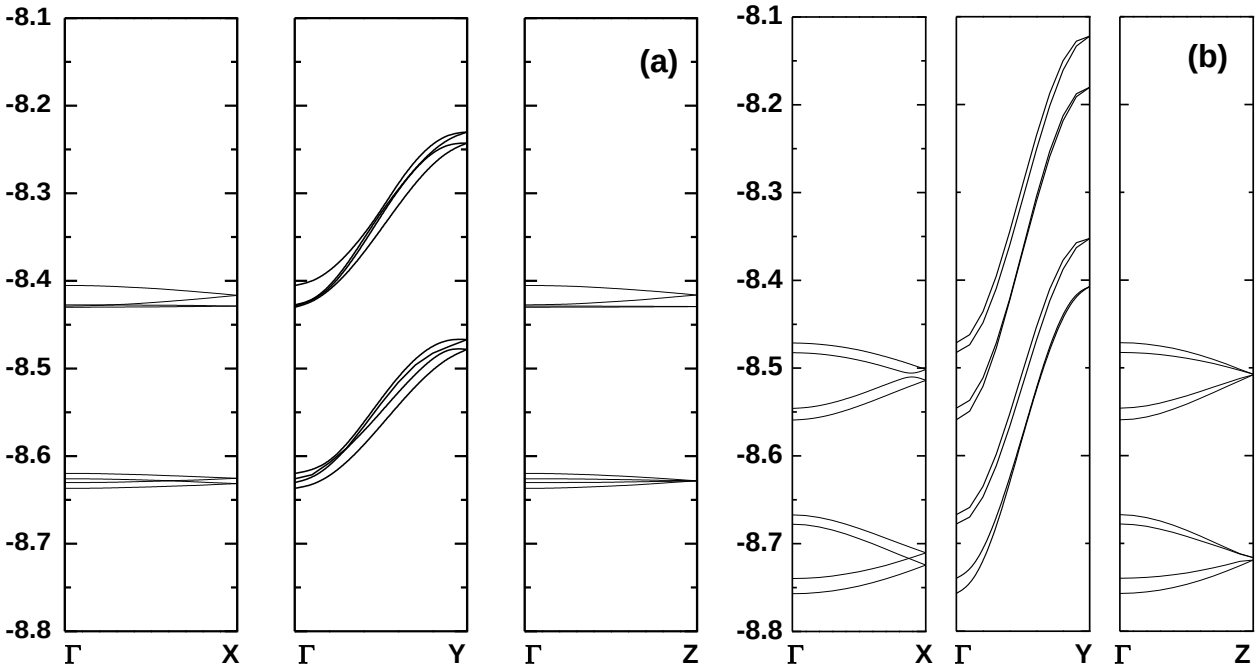

The combination of electrical and magnetic properties observed for **11** is typical of a Mott insulator [57–59], in which the unpaired spins are localized due to dominance of the Coulomb interaction U over the transfer integral t. Thus the magnetic data are well described in terms of a one dimensional $S = 1/2$ antiferromagnetic Heisenberg chain with $J = 6.3$ cm^{-1} (Figure 7) [55]. The non-metallic character of the conductivity (Figure 8) would then be result of the localization of unpaired electrons due to their Coulombic repulsion as a result of the large intermolecular separation [57–59].

3. Experimental Section

3.1. Materials

All reactions and manipulations were carried out under an atmosphere of dry argon using standard Schlenk and vacuum-line techniques. 9-hydroxy-1-oxophenalenone was synthesized according to literature procedure [60]. Cyclohexanemethyllamine (Aldrich), boron trichloride (Aldrich), sodium tetraphenylborate (Aldrich), and cobaltocene (Strem) were used as received. Solvents were dried and distilled according to standard procedures immediately before use. The NMR spectra were recorded on a Bruker 300 spectrometer. Mass spectra (MALDI) were run on a Voyager-DE STR BioSpectrometry Workstation mass spectrometer. Elemental analyses were performed by the Microanalysis Laboratory, University of Illinois, Urbana, IL.

3.2. Preparation of NCH_2CyHx, O-PLY

A mixture of 9-hydroxyphenalenone (0.98 g, 0.005 mol), cyclohexanemethylamine (5 g, 0.044 mol) and 15 mL of water were heated to 145 °C in a heavy-walled sealed tube for 48 h. The mixture was allowed to cool, the tube was vented and opened, and the contents poured into 150 mL of distilled water. The aqueous mixture was extracted with 200 mL chloroform. The organic layer was washed repeatedly with water and dried over anhydrous sodium sulfate. The solvent was removed under reduced pressure to give a yellow solid. The crude product was purified by column chromatography on Al_2O_3 with $CHCl_3$ to give a yellow solid. Recrystallization from a methanol and dichloromethane mixture gave 1.16 g (80 %) of the desired compound. m.p. 71–74 °C; ^{1}H NMR (300 MHz, $CDCl_3$, 25 °C): δ 12.43 (s, 1H), 8.99 (d, 1H, J = 9.40 Hz), 7.90–7.84 (m, 3H), 7.43 (t, 1H, J = 7.60 Hz), 7.23 (d, 1H, J = 9.40 Hz), 7.01 (d, 1H, J = 9.60 Hz), 3.42 (t, 2H, J = 6.30 Hz), 1.98–1.94 (m, 2H), 1.84–1.70 (m, 4H), 1.38–1.10 (m, 5H). HRMS (ESI) m/z calcd. for $C_{20}H_{22}NO$ [MH^+] 292.3948. found. 292.3954. Anal. calcd for $C_{20}H_{22}NO$: C 82.44; H 7.26; N 4.81 %. Found. C 82.49; H 7.20; N 4.83.

*3.3. Preparation of $[(NCH_2CyHx,O\text{-}PLY)_2B]^+BPh_4^-$ (**11**$^+BPh_4^-$)*

A solution of 9-cyclohexanemethylamino-1-oxo-phenalenone (0.58 g, 2 mmol) in dry 1,2-dichloroethane (20 mL) was treated with boron trichloride (1 mL, 1M solution in hexane) under argon. The mixture was stirred for 72 h at 70 ℃ temperature. The yellow solution of the ligand became dark red in color upon addition of boron trichloride. Solvent was removed by rotary evaporator and the semi-solid mass was dissolved in 25 mL of dry methanol. To it methanol solution (25 mL) of sodium tetraphenyl borate (1.03 g, 3 mmol) was added in stirring condition. Yellow–orange solid deposited was filtered and the solid was washed with excess of methanol, dried in vacuum. Yield: 0.55 g (60 %) m.p. 117–118 °C; ^{1}H NMR (300 MHz, $CDCl_3$, 25 °C): 8.40 (d, 2H, J = 9.12 Hz), 8.24 (d, 2H, J = 8.13 Hz), 8.08 (d, 2H, J = 9.55 Hz), 8.03 (d, 2H, J = 6.21 Hz), 7.77 (t, 2H, J = 7.85 Hz), 7.44 (t, 8H, J = 8.47 Hz), 7.36 (d, 2H, J = 6.21 Hz), 7.07 (d, 2H, J = 6.21 Hz), 7.00 (t, 8H, J = 7.37 Hz), 6.83 (t, 4H, J = 7.11 Hz), 3.46 (d, 2H, J = 6.21 Hz), 2.83 (d, 2H, J = 6.21 Hz), 1.68–1.55 (m, 5H), 1.10–0.90 (m, 4H), 0.80–0.69 (m, 2H). MALDI MS m/z calcd. for $C_{40}H_{40}BN_2O_2^+$ [M^+] 591. found. 591. Anal. calcd for $C_{64}H_{60}B_2N_2O_2$: C 84.40, H 6.64, N 3.08 %. Found. C 83.97, H 6.42, N 3.20.

*3.4. Crystallization of $[(NCH_2CyHx,O\text{-}PLY)_2B]^\bullet$ (**11**)*

A solution of 175 mg (1.92×10^{-4} mol) of **11**$^+BPh_4^-$ in 20 mL of dry acetonitrile was placed in a 30 mL sample vial, and 75 mg (3.9×10^{-4} mol) of $CoCp_2$ in 10 mL of dry acetonitrile was placed in another 20 mL sample vial. Cobaltocene solution was added slowly to the sample solution and the whole mixture was kept undisturbed inside glove box. After sitting in the dark for 4 days, 55 mg of black shining needle like crystals of radical were isolated. Yield; 49 %. m.p. 198 °C (decomposition temperature) Anal. calcd for $C_{40}H_{40}BN_2O_2$: C 81.21, H 6.82, N 4.74 %. Found. C 80.80, H 6.73, N 4.79.

3.5. Cyclic Voltammetry

Electrochemical measurements were performed using a CH Instruments Electrochemical Analyzer, with scan rates of 100 mV/s, on solutions (10^{-3} M) of $\mathbf{11}^{+}BPh_4^{-}$ in oxygen-free acetonitrile (distilled from CaH_2), containing 0.1 M tetra-*n*-butylammonium hexafluorophosphate. Potentials were scanned with respect to the saturated calomel reference electrode in a single-compartment cell fitted with Pt electrodes and referenced to the Fc/Fc^{+} couple of ferrocene at 0.38 V *vs*. SCE.

3.6. X-ray Crystallography

A black thin needle fragments was used for the single crystal *x*-ray diffraction study of $C_{40}H_{40}BN_2O_2$ (**11**). The crystals were mounted on to a cryo-loop glass fiber with paratone oil. X-ray intensity data were collected on a Bruker APEX2 (version 2.0-22) [61] platform-CCD X-ray diffractometer system (Mo-radiation, λ = 0.71073 Å, 50 KV/40 mA power). The CCD detector was placed at a distance of 5.0550 cm from the crystal. The frames were integrated using the Bruker SAINT software package (version V7.23A) [62,63] and using a narrow-frame integration algorithm. Absorption corrections were applied to all the raw intensity data using the SADABS program [64]. Atomic coordinates, isotropic and anisotropic displacement parameters of all the non-hydrogen atoms were refined by means of a full matrix least-squares procedure on F^2. The H-atoms were included in the refinement in calculated positions riding on the atoms to which they were attached. The CIF file is provided in the Supporting Information.

3.7. Magnetic Susceptibility Measurements

Magnetic susceptibility measurement for **11** was performed over the temperature range 4.4–330 K on a George Associates Faraday balance operating at 0.5 T. The system was calibrated using Al and Pt NIST standards.

3.8. Conductivity Measurements

The single-crystal conductivity (σ), of **11** was measured for a crystal (Figure S2) in a four-probe configuration using in-line contacts which were attached with silver paint. The needle-like crystals were freely positioned on a sapphire substrate, and the electrical connections between the silver paint contacts on the crystal and the indium pads on the substrate were made by thin, flexible 25 μm diameter silver wires to relieve mechanical stress during thermal cycling of the crystal. The temperature dependence of the conductivity was measured in the range 330–80 K using a custom made helium variable temperature probe with a Lake Shore 340 temperature controller driven by LabVIEW software. A Keithley 236 unit was used as a voltage source and current meter, and two 6517A Keithley electrometers were used to measure the voltage drop between the potential leads in a four-probe configuration.

3.9. Single-Crystal Near- and Mid-Infrared Transmission Spectroscopy

The infrared transmission measurements were carried out in a FTIR Nicolet Nexus 670 ESP spectrometer integrated with Continuum Thermo-Nicolet FTIR microscope.

3.10. Band Structure Calculations

The band structure calculations made use of a modified version of the extended Hückel theory (EHT) band structure program [65–67], as described previously [47,68,69]. The parameter set is chosen to provide a reasonably consistent picture of bonding in heterocyclic organic compounds [70,71].

3.11. Electron Paramagnetic Resonance Spectroscopy

The electron paramagnetic resonance spectrum (Figure S1) of compound **11** was measured on a BrukerEMX EPR spectrometer.

4. Conclusions

By changing the substituent at the 9-position to cyclohexanemethylamine, another entrant into the series of $[PLY(O, NR)]_2B$ radicals has been synthesized, characterized and its solid state properties have been investigated. The disproportionation energy, which determines the on-site Coulomb correlation energy in the solid state is very similar to the alkyl substituted spiro-bis(1,9-substituted phenalenyl)boron neutral radicals reported earlier. In the solid state, the radical is not strictly monomeric nor does it form isolated σ- or π-dimers, and the structure shows that these radicals pack in a continuous array of π-step neighboring PLY units. The magnetic susceptibility indicates that there is significant spin–spin interaction between the molecules, but the relatively large separation between the spin-bearing carbons and the on-site Coulomb correlation energy together limit the room temperature conductivity to a value $\sigma_{RT} = 2.4 \times 10^{-3}$ S/cm.

Conflict of Interest

The authors declare no conflict of interest.

Acknowledgements

This work was supported by the Office of Basic Energy Sciences, U.S. Department of Energy under grant no. DE-FG02-04ER46138.

References

1. Wolf, S.A.; Awschalom, D.D.; Buhrman, R.A.; Daughton, J.M.; von Molnar, S.; Roukes, M.L.; Chtchelkanova, A.Y.; Treger, D.M. Spintronics: A spin-based electronics vision for the future. *Science* **2001**, *294*, 1488–1495.
2. Matsushita, M.M.; Kawakami, H.; Kawada, Y.; Sugawara, T. Negative magnetoresistance observed on an ion radical salt of a TTF-based spin polarized donor. *Chem. Lett.* **2007**, *36*, 110–111.
3. Matsushita, M.M.; Kwakami, H.; Sugawara, T.; Ogata, M. Molecule-based system with coexisting conductivity and magnetism and without magnetic inorganic ions. *Phys. Rev. B* **2008**, *77*, 195208–195213.

4. Takahide, Y.; Konoike, T.; Enomoto, K.; Nishimura, M.; Terashima, T.; Uji, S.; Yamamoto, H.M. Large positive magnetoresistance of insulating organic crystals in the non-ohmic region. *Phy. Rev. Lett.* **2007**, *98*, 116602–116605.
5. Dediu, V.A.; Hueso, L.E.; Bergenti, I.; Taliani, C. Spin routes in organic semiconductors. *Nat. Mater*. **2009**, *8*, 707–716.
6. Hicks, R.G. What's new in stable radical chemistry? *Org. Biomol. Chem.* **2007**, *5*, 1321–1338.
7. Hicks, R.G. A new spin on bistability. *Nat. Chem.* **2011**, *3*, 189–191.
8. Morita, Y.; Nishida, S. Stable radicals: Fundamentals and applied aspects of odd-electron compounds. In *Phenalenyls, Cyclopentadienyls, and Other Carbon-Centered Radicals*; Hicks, R.G., Ed.; John Wiley & Sons: West Suxxes, UK, 2010, pp: 83–132.
9. Reid, D.H. Syntheses and properties of the perinaphthyl radical. *Chem. Ind.* **1956**, 1504–1505.
10. Reid, D.H. The chemistry of the phenalenes. *Quart. Rev.* **1965**, *19*, 274–302.
11. Morita, Y.; Suzuki, S.; Sato, K.; Takui, T. Synthetic organic spin chemistry for structurally well-defined open-shell graphene fragments. *Nat. Chem.* **2011**, *3*, 197–204.
12. Morita, Y.; Suzuki, S.; Fukui, K.; Nakazawa, S.; Kitagawa, H.; Kishida, H.; Okamoto, H.; Naito, A.; Sekine, A.; Ohashi, Y.; *et al.* Thermochromism in an organic crystal based on the coexistance of σ- and π-dimers. *Nat. Mater.* **2008**, *7*, 48–51.
13. Haddon, R.C. Design of organic metals and superconductors. *Nature* **1975**, *256*, 394–396.
14. Haddon, R.C. Quantum chemical studies in the design of organic metals. III. Odd-alternant hydrocarbons (OAHs): The phenalenyl (PLY) system. *Aust. J. Chem.* **1975**, *28*, 2343–2351.
15. Haddon, R.C. Quantum chemical studies in the design of organic metals. II. The equilibrium geometries and electronic structure of tetrathiafulvalene (TTF) and tetracyanoquinodimethane (TCNQ) and their uni- and di-valent ions. *Aust. J. Chem.* **1975**, *28*, 2333–2342.
16. Goto, K.; Kubo, T.; Yamamoto, K.; Nakasuji, K.; Sato, K.; Shiomi, D.; Takui, T.; Kubota, M.; Kobayashi, T.; Yakusi, K.; *et al.* A stable neutral hydrocarbon radical: Synthesis, crystal structure, and physical properties of 2,5,8-tri-tert-butyl-phenalenyl. *J. Am. Chem. Soc.* **1999**, *121*, 1619–1620.
17. Morita, Y.; Aoki, T.; Fukui, K.; Nakazawa, S.; Tamaki, K.; Suzuki, S.; Fuyuhiro, A.; Yamamoto, K.; Sato, K.; Shiomi, D.; *et al.* A new trend in phenalenyl chemistry: A persistent neutral radical, 2,5,8-tri-tert-butyl-1,3-diazaphenalenyl, and the excited triplet state of the gable *syn*-dimer in the crystal of column motif. *Angew. Chem. Int. Ed.* **2002**, *41*, 1793–1796.
18. Morita, Y.; Nishida, S.; kawai, J.; Takui, T.; Nakasuji, K. Oxophenalenoxyl: Novel stable neutral radicals with a unique spin-delocalized nature depending on topological symmetries and redox states. *Pure Appl. Chem.* **2008**, *80*, 507–517.
19. Koutentis, P.A.; Chen, Y.; Cao, Y.; Best, T.P.; Itkis, M.E.; Beer, L.; Oakley, R.T.; Brock, C.P.; Haddon, R.C. Perchlorophenalenyl radical. *J. Am. Chem. Soc.* **2001**, *123*, 3864–3871.
20. Fukui, K.; Sato, K.; Shiomi, D.; Takui, T.; Itoh, K.; Gotoh, K.; Kubo, T.; Yamamoto, K.; Nakasuji, K.; Naito, A. Electronic structure of a stable phenalenyl radical in crystalline state as studied by squid measurements, cw-esr, and ^{13}C cp/mas nmr spectroscopy. *Synth. Met.* **1999**, *103*, 2257–2258.

21. Small, D.; Zaitsev, V.; Jung, Y.; Rosokha, S.V.; Head-Gordon, M.; Kochi, J.K. Intermolecular π to π bonding between stacked aromatic dyads. Experimental and theoretical binding energies and near-ir optical transitions for phenalenyl radical/radical versus radical/cation dimerizations. *J. Am. Chem. Soc.* **2004**, *126*, 13850–13858.
22. Zheng, S.; Lan, J.; Khan, S.I.; Rubin, Y. Synthesis, characterization, and coordination chemistry of the 2-azaphenalenyl radical. *J. Am. Chem. Soc.* **2003**, *125*, 5786–5791.
23. Zheng, S.; Thompson, J.D.; Tontcheva, A.; Khan, S.I.; Rubin, Y. Perchloro-2,5,8-triazaphenalenyl radical. *Org. Lett.* **2005**, *7*, 1861–1863.
24. Haddon, R.C.; Wudl, F.; Kaplan, M.L.; Marshall, J.H.; Cais, R.E.; Bramwell, F.B. 1,9-dithiophenalenyl system. *J. Am. Chem. Soc.* **1978**, *100*, 7629–7633.
25. Beer, L.; Reed, R.W.; Robertson, C.M.; Oakley, R.T.; Tham, F.S.; Haddon, R.C. Tetrathiophenalenyl radical and its disulfide-bridged dimer. *Org. Lett.* **2008**, *10*, 3121–3123.
26. Beer, L.; Mandal, S.K.; Reed, R.W.; Oakley, R.T.; Tham, F.S.; Donnadieu, B.; Haddon, R.C. The first electronically stabilized phenalenyl radical: Effect of substituents on solution chemistry and solid state structure. *Cryst. Growth Design* **2007**, *7*, 802–809.
27. Parkin, S.S.P.; Engler, E.M.; Schumaker, R.R.; Lagier, R.; Lee, V.Y.; Scott., J.C.; Greene, R.L. Superconductivity in a new family of organic conductors. *Phys. Rev. Lett.* **1983**, *50*, 270–273.
28. Haddon, R.C.; Hebard, A.F.; Rosseinsky, M.J.; Murphy, D.W.; Duclos, S.J.; Lyons, K.B.; Miller, B.; Rosamilia, J.M.; Fleming, R.M.; Kortan, A.R.; *et al.* Conducting films of C_{60} and C_{70} by alkali metal doping. *Nature* **1991**, *350*, 320–322.
29. Pal, S.K.; Itkis, M.E.; Tham, F.S.; Reed, R.W.; Oakley, R.T.; Haddon, R.C. Resonating valence-bond ground state in a phenalenyl-based neutral radical conductor. *Science* **2005**, *309*, 281–284.
30. Bag, P.; Itkis, M.E.; Pal, S.K.; Donnadieu, B.; Tham, F.S.; Park, H.; Schleuter, J.A.; Siegrist, T.; Haddon, R.C. Resonating valence bond and sigma-charge density wave phases in a benzannulated phenalenyl radical. *J. Am. Chem. Soc.* **2010**, *132*, 2684–2694.
31. Robertson, C.M.; Leitch, A.A.; Cvrkalj, K.; Myles, D.J.T.; Reed, R.W.; Dube, P.A.; Oakley, R.T. Ferromagnetic ordering in bisthiaselenazoyl radicals: Variations on a tetragonal theme. *J. Am. Chem. Soc.* **2008**, *130*, 14791–14801.
32. Leitch, A.A.; Lekin, K.; Winter, S.M.; Downie, L.E.; Tsuruda, H.; Tse, J.S.; Mito, M.; Desgreniers, S.; Dube, P.A.; Zhang, S.; *et al.* From magnets to metals: The response of tetragonal bisdiselenazolyl radicals to pressure. *J. Am. Chem. Soc.* **2011**, *133*, 6051–6060.
33. Winter, S.M.; Datta, S.; Hill, S.; Oakley, R.T. Magnetic anisotropy in a heavy atom radical ferromagnet. *J. Am. Chem. Soc.* **2011**, *133*, 8126–8129.
34. Yu, X.; Mailman, A.; Dube, P.A.; Assoud, A.; Oakley, R.T. The first semiquinone-bridged bisdithiazolyl radical conductor: A canted antiferromagnet displaying a spin-flop transition. *Chem. Commun.* **2011**, *47*, 4655–4657.
35. Yu, X.; Mailman, A.; Lekin, K.; Assoud, A.; Robertson, C.M.; Noll, B.C.; Campana, C.F.; Howard, J.A.K.; Dube, P.A.; Oakley, R.T. Semiquinone-bridged bisdithiazoyl radicals as neutral radical conductors. *J. Am. Chem. Soc.* **2012**, *134*, 2264–2275.

36. Chi, X.; Itkis, M.E.; Patrick, B.O.; Barclay, T.M.; Reed, R.W.; Oakley, R.T.; Cordes, A.W.; Haddon, R.C. The first phenalenyl-based neutral radical molecular conductor. *J. Am. Chem. Soc.* **1999**, *121*, 10395–10402.
37. Mandal, S.K.; Itkis, M.E.; Chi, X.; Samanta, S.; Lidsky, D.; Reed, R.W.; Oakley, R.T.; Tham, F.S.; Haddon, R.C. New family of aminophenalenyl-based neutral radical molecular conductors: Synthesis, structure, and solid state properties. *J. Am. Chem. Soc.* **2005**, *127*, 8185–8196.
38. Chi, X.; Itkis, M.E.; Kirschbaum, K.; Pinkerton, A.A.; Oakley, R.T.; Cordes, A.W.; Haddon, R.C. Dimeric phenalenyl-based neutral radical molecular conductors. *J. Am. Chem. Soc.* **2001**, *123*, 4041–4048.
39. Itkis, M.E.; Chi, X.; Cordes, A.W.; Haddon, R.C. Magneto-opto-electronic bistability in a phenalenyl-based neutral radical. *Science* **2002**, *296*, 1443–1445.
40. Miller, J.S. Bistable electrical, optical, and magnetic behavior in molecule-based material. *Angew. Chem. Int. Ed.* **2003**, *42*, 27–29.
41. Huang, J.; Kertesz, M. Spin crossover of spiro-biphenalenyl neutral radical molecular conductors. *J. Am. Chem. Soc.* **2003**, *125*, 13334–13335.
42. Huang, J.; Kertesz, M. Theoritical analysis of intermolecular covalent π-π bonding and magnetic properties of phenalenyl and spiro-biphenalenyl radical pi-dimers. *J. Phys. Chem. A* **2007**, *111*, 6304–6315.
43. Chi, X.; Itkis, M.E.; Reed, R.W.; Oakley, R.T.; Cordes, A.W.; Haddon, R.C. Conducting pathways in organic solids: A phenalenyl-based neutral radical of low conductivity. *J. Phys. Chem. B* **2002**, *106*, 8278–8287.
44. Chi, X.; Itkis, M.E.; Tham, F.S.; Oakley, R.T.; Cordes, A.W.; Haddon, R.C. Synthesis, structure and physical properties of a new phenalenyl-based neutral radical crystal: Correlation between structure and transport properties in carbon-based molecular conductors. *Int. J. Quant. Chem.* **2003**, *95*, 853–865.
45. Liao, P.; Itkis, M.E.; Oakley, R.T.; Tham, F.S.; Haddon, R.C. Light-mediated c-c sigma-bond driven crystallization of a phenalenyl radical dimer. *J. Am. Chem. Soc.* **2004**, *126*, 14297–14302.
46. Pal, S.K.; Itkis, M.E.; Tham, F.S.; Reed, R.W.; Oakley, R.T.; Haddon, R. Trisphenalenyl-based neutral radical molecular conductor. *J. Am. Chem. Soc.* **2008**, *130*, 3942–3951.
47. Pal, S.K.; Itkis, M.E.; Tham, F.S.; Reed, R.W.; Oakley, R.T.; Donnadieu, B.; Haddon, R.C. Phenalenyl-based neutral radical molecular conductors: Substituent effects on solid-state structures and properties. *J. Am. Chem. Soc.* **2007**, *129*, 7163–7174.
48. Pal, S.K.; Itkis, M.E.; Reed, R.W.; Oakley, R.T.; Cordes, A.W.; Tham, F.S.; Siegrist, T.; Haddon, R.C. Synthesis, structure and physical properties of the first one-dimensional phenalenyl-based neutral radical conductor. *J. Am. Chem. Soc.* **2004**, *126*, 1478–1484.
49. Pauling, L. The metallic state. *Nature* 1948, *161*, 1019–1020.
50. Anderson, P.W. Resonating valence bonds: A new kind of insulator? *Mater. Res. Bull.* **1973**, *8*, 153–160.
51. Mandal, S.K.; Samanta, S.; Itkis, M.E.; Jensen, D.W.; Reed, R.W.; Oakley, R.T.; Tham, F.S.; Donnadieu, B.; Haddon, R.C. Resonating valence bond ground state in oxygen-functionalized phenalenyl-based neutral radical conductors. *J. Am. Chem. Soc.* **2006**, *128*, 1982–1994.

52. Sarkar, A.; Pal, S.K.; Itkis, M.E.; Liao, P.; Tham, F.S.; Donnadieu, B.; Haddon, R.C. Methoxy-substituted phenalenyl-based neutral radical molecular conductor. *Chem. Mater.* **2009**, *21*, 2226–2237.
53. Sarkar, A.; Itkis, M.E.; Tham, F.S.; Haddon, R.C. Synthesis, structure, and physical properties of a partial pi-stacked phenalenyl-based neutral radical molecular conductor. *Chem. Eur. J.* **2011**, *17*, 11576–11584.
54. Robbins, J.L.; Edelstein, N.; Spencer, B.; Smart, J.C. Syntheses and electronic structure of decamethylmetallocenes. *J. Am. Chem. Soc.* **1982**, *104*, 1882–1893.
55. Bonner, J.C.; Fisher, M.E. Linear magnetic chains with anisotropic coupling. *Phys. Rev.* **1964**, *135*, A640–A658.
56. Estes, W.E.; Gavel, D.P.; Hatfield, W.E.; Hodgson, D.J. Magnetic and structural characterization of dibromo- and dichlorobis(thiazole)copper(II). *Inorg. Chem.* **1978**, *17*, 1415–1421.
57. Mott, N.F. *Metal-insulator transitions*, 2nd ed.; CRC Press: Boca Raton, FL, USA, 1990.
58. Yoneyama, N.; Miyazaki, A.; Enoki, T.; Saito, G. Magnetic properties of ttf-type charge transfer salts in mott insulator regime. *Bull. Chem. Soc. Jpn.* **1999**, *72*, 639–651.
59. Whangbo, M.-H.; Hoffmann, R.; Woodward, R.B. Conjugated one and two dimensional polymers. *Proc. Royal Soc. Lond. A* **1979**, *366*, 23–46.
60. Haddon, R.C.; Chichester, S.V.; Mayo, S.L. Direct amination of 9-hydroxyphenalenone to produce 9-aminophenalenone and related compounds. *Synthesis* **1985**, 639–641.
61. *Apex 2*, 2009.5-1 version; Bruker AXS Inc.: Madison, WI, USA, 2009.
62. *Saint Software Reference Manual*, V7.23A; Bruker Analytical X-Ray System Inc: Madison, WI, USA, 2003.
63. *Shelxtl*, 2008/4 version; Bruker AXS Inc.: Madison, WI, USA, 2008.
64. *Sadabs*, 2008/1 version; Bruker AXS Inc.: Madison, WI, USA, 2008.
65. Hoffmann, R. An extended Hückel theory. I. Hydrocarbons. *J. Chem. Phys.* **1963**, *39*, 1397–1412.
66. Hofmann, R. *Solids and surfaces*; Wiley-VCH: Minnesota, MN, USA, 1988.
67. Whangbo, M.H. Mott-hubbard condition for electronic localization in the hartee-fock band theory. *J. Chem. Phys.* **1979**, *70*, 4963–4966.
68. Haddon, R.C.; Siegrist, T.; Fleming, R.M.; Bridenbaugh, P.M.; Laudise, R.A. Band structures of organic thin-film transistor materials. *J. Mater. Chem.* **1995**, *5*, 1719–1724.
69. Haddon, R.C.; Chi, X.; Itkis, M.E.; Anthony, J.E.; Eaton, D.L.; Siegrist, T.; Mattheus, C.C.; Palstra, T.T.M. Band electronic structure of one- and two-dimensional pentacene molecular crystals. *J. Phys. Chem. B* **2002**, *106*, 8288–8292.
70. Andrews, M.P.; Cordes, A.W.; Douglass, D.C.; Fleming, R.M.; Glarum, S.H.; Haddon, R.C.; Marsh, P.; Oakley, R.T.; Palstra, T.T.M.; Schneemeyer, L.F.; *et al.* One-dimensional stacking of bifunctional dithia- and diselena-diazolyl radicals: Preparation and structural and electronic properties of 1,3-[(E_2N_2C)C_6H_4(CN_2E_2)](E = S, Se). *J. Am. Chem. Soc.* **1991**, *113*, 3559–3568.

71. Cordes, A.W.; Haddon, R.C.; Oakley, R.T.; Schneemeyer, L.F.; Waszczak, J.V.; Young, K.M.; Zimmerman, N.M. Molecular semiconductors from bifunctional dithia- and diselenadiazolyl radicals. Preparation and solid-state structural and electronic properties of 1,4-[(E_2N_2C)C_6H_4(CN_2E_2)] (E = S,Se). *J. Am. Chem. Soc.* **1991**, *113*, 582–588.